INTERNATIONAL JOURNAL OF PHARMACEUTICAL SCIENCES
[ISSN: 0975-4725; CODEN(USA): IJPS00]
Journal Homepage: https://www.ijpsjournal.com

Research Article

To Develop and Optimize *Bacopa monnieri* in Situ Thermosensitive Hydrogel for The Treatment of Acute Wound Healing

Pratima Sagar*, Sharavari Chavan, Dr. Hemlata Wadkar, Dr. Varsha Patil, Dr. Trupti Tuse

Abhinav College of Pharmacy, Mokarwadi, Narhe, Pune, Maharashtra 411041, India.

ARTICLE INFO

Published: 01 Sept 2026
Keywords:
pharmacovigilance, adverse drug reactions, preventability, Schumock and Thornton scale, predictors, India, secondary data analysis
DOI:
10.5281/zenodo.22247225

ABSTRACT

Conventional topical wound-care systems remain limited by poor site retention, uneven application, and reliance on synthetic active agents that can irritate already compromised tissue, creating a clear need for phytotherapeutic alternatives capable of sustained, site-specific delivery. The present study aimed to develop and optimize a thermosensitive in-situ hydrogel incorporating Bacopa monnieri for the treatment of acute wounds. A UV spectrophotometric method was first validated for the extract, confirming a sharp absorbance maximum and a linear calibration curve in accordance with the Beer–Lambert law. The hydrogel was optimized using Poloxamer 407 and HPMC K4M as the independent polymeric variables, from which three representative batches (F1–F3) were prepared and characterized for pH, viscosity, gelation temperature, gelling time, spreadability, and mucoadhesive strength. Batch F3 was selected as the optimized formulation on the basis of its balanced gelation temperature (35.8 °C) and good mucoadhesive strength (3680 dyne/cm²), together with superior functional performance. In vitro drug diffusion studies using a Franz diffusion cell showed that F3 achieved the highest cumulative drug release (97.5% at 24 h), indicating a sustained-release profile. Molecular docking of the major phytoconstituents, Bacoside A and Bacoside B, against the angiogenesis-related receptor VEGFR-2 (validated with an RMSD of 0.5 Å) revealed favourable binding interactions, with Bacoside A showing the stronger profile. Antimicrobial evaluation confirmed activity against both Escherichia coli and Streptococcus spp., supporting the formulation's potential as a multifunctional, phytotherapeutic wound-healing platform.

INTRODUCTION

1.1 Wound Healing Physiology

The skin, as the body's largest and most exposed organ, possesses a remarkable intrinsic capacity for repair following injury. Wound healing is

***Corresponding Author:** Pratima Sagar
Address: *Abhinav College of Pharmacy, Mokarwadi, Narhe, Pune, Maharashtra 411041, India.*
Email ✉: pratimasagar13@gmail.com
Relevant conflicts of interest/financial disclosures: The authors declare that the research was conducted in the absence of any commercial or financial relationships that could be construed as a potential conflict of interest.

classically described as a dynamic, overlapping sequence of four physiological phases hemostasis, inflammation, proliferation, and remodeling each dependent on the successful completion of the one preceding it[1]. The hemostatic phase begins within seconds of tissue injury, as vasoconstriction and platelet aggregation act to arrest bleeding at the wound site. Activated platelets release a range of bioactive mediators, most notably platelet-derived growth factor (PDGF) and transforming growth factor-beta (TGF-β), which recruit immune cells and set the stage for subsequent healing events[1,2,3]. Concurrently, activation of the coagulation cascade converts fibrinogen to fibrin, forming a stabilizing clot that also serves as a provisional scaffold for cell migration[2].

Following hemostasis, the wound enters the inflammatory phase, typically lasting 24–72 hours, during which neutrophils and later macrophages infiltrate the wound bed to clear pathogens and necrotic tissue. Macrophages, in particular, play a dual regulatory role first as pro-inflammatory effectors and later transitioning to a reparative phenotype that secretes anti-inflammatory cytokines and angiogenic factors such as vascular endothelial growth factor (VEGF), thereby bridging the inflammatory and proliferative stages[3]. The proliferative phase, spanning roughly days 3–10 post-injury, is marked by fibroblast proliferation, collagen deposition, and angiogenesis driven substantially by VEGF-mediated neovascularization, alongside re-epithelialization of the wound surface by migrating keratinocytes[4,5,6,7]. Finally, the remodeling (or maturation) phase which may extend from several weeks to over a year involves the enzymatic replacement of immature type III collagen with more organized, cross-linked type I collagen, regulated by matrix metalloproteinases (MMPs) and their tissue inhibitors (TIMPs)[8,9]. This phase restores the mechanical strength of the healed tissue, although typically only to 70–80% of that of uninjured skin[5]. A clear understanding of this staged, mediator-driven process underscores why therapeutic strategies targeting moisture retention, sustained bioactive delivery, and pro-angiogenic support at the wound site hold particular promise for enhancing healing outcomes[10].

1.2 Limitations of Conventional Wound Care and the Rationale for In-Situ Hydrogels

Despite the well-characterized biology of wound repair, conventional topical wound-care modalities including ointments, creams, and traditional dressings continue to present significant practical limitations. These formulations are frequently associated with poor retention at the wound site, necessitating repeated reapplication; uneven distribution of the active agent across the wound surface; and an inability to adequately regulate moisture balance, a factor now recognized as critical to efficient re-epithelialization and fibroblast activity. Additionally, many conventional products rely on synthetic active agents that may provoke irritation or sensitization with prolonged use, particularly in already compromised tissue.

These shortcomings have driven growing interest in advanced topical drug delivery platforms capable of site-specific, controlled, and sustained release. Among these, in-situ forming hydrogels have emerged as a particularly promising approach. Such systems exist as free-flowing liquids at room temperature, allowing for straightforward, precise application, and subsequently undergo a sol-to-gel phase transition upon contact with the skin at physiological temperature. The resulting gel adheres closely to the wound bed, prolonging formulation contact time and enabling sustained release of the incorporated therapeutic agent, while

simultaneously maintaining the moist wound environment associated with enhanced granulation tissue formation and re-epithelialization. Thermosensitive hydrogel systems, built typically upon polymers such as Poloxamer 407 in combination with bioadhesive agents like HPMC K4M, offer the additional advantage of gelling specifically at body temperature, eliminating the need for external triggers or mechanical fixation and improving patient comfort, application precision, and overall compliance advantages that are especially valuable in wounds located at mobile or difficult-to-dress anatomical sites[11,12,13].

1.3 Bacopa monnieri as a Phytotherapeutic Candidate

In parallel with innovations in formulation science, there has been increasing interest in incorporating plant-derived bioactive compounds into modern wound-care systems, owing to their generally favorable safety profiles and multifunctional pharmacological activity relative to synthetic alternatives. *Bacopa monnieri* (commonly known as Brahmi) is a phytoconstituent traditionally recognized for its neuroprotective and cognitive-enhancing properties, but more recent investigations have highlighted its antioxidant, anti-inflammatory, and antimicrobial activities properties directly relevant to the management of cutaneous injury[14,15,16]. Its principal bioactive constituent, Bacoside A, has been shown to modulate inflammatory cytokine levels, scavenge free radicals, and stimulate fibroblast proliferation and collagen synthesis, each of which contributes meaningfully to wound closure and tissue remodeling. Bacoside A has additionally been reported to promote angiogenesis and support granulation tissue formation, reinforcing its potential relevance to the proliferative phase of dermal repair[17,18,19].

Notably, while the neuropharmacological properties of *Bacopa monnieri* have been extensively studied, its application in cutaneous wound healing and particularly its incorporation into a modern, thermoresponsive drug delivery platform remains a comparatively underexplored area of research. This represents a meaningful gap in the phytotherapeutic literature, given the plant's demonstrated multifunctional bioactivity and its compatibility with the broader clinical shift toward natural, patient-centric wound-care solutions[20,21,22].

1.4 Research Gap, Aim, and Objectives

Taken together, the limitations of existing topical wound-care systems and the underutilized therapeutic potential of *Bacopa monnieri* in dermal applications point to a clear opportunity: the development of a thermosensitive in-situ hydrogel that combines the delivery advantages of modern polymeric systems with the multifunctional bioactivity of this well-characterized phytoconstituent. Such a formulation could offer sustained, localized delivery of *Bacopa monnieri* directly to the wound site, while minimizing systemic exposure and preserving the compound's inherent antioxidant, anti-inflammatory, and antimicrobial properties[23,24].

Accordingly, the present study was designed to develop and optimize a *Bacopa monnieri* in-situ thermosensitive hydrogel for the effective treatment of acute wound healing. The specific objectives of the study were: (i) to formulate an in-situ thermosensitive hydrogel suitable for topical application; (ii) to optimize the formulation parameters, using a factorial design approach, for enhanced drug stability and release; (iii) to perform molecular docking studies to evaluate the potential wound-healing-related bioactivity of the formulation's phytoconstituents; (iv) to

characterize the physicochemical properties of the optimized hydrogel, including its viscosity, gelation temperature, and spreadability; and (v) to assess the in vitro drug release profile and antimicrobial efficacy of the developed formulation[25,26].

2. MATERIALS AND METHODS:

2.1 Materials and Equipment

Bacopa monnieri was procured from Dhanvantari Ayurvedalaya, Bibwewadi, Pune, India. Poloxamer 407 and HPMC K4M were obtained from Sciquant Innovations (OPC) Pvt. Ltd., Pune, India. Methanol, ethanol (99.7%), and DMSO were of analytical grade, procured locally; phosphate buffer (pH 6.8) was laboratory-prepared using analytical-grade reagents. Potassium bromide (KBr) was sourced from Shimadzu, Japan, and distilled water was laboratory-purified and used throughout, including for the Franz diffusion cell studies. Materials and equipment are summarized in Table 1.

Table 1. Materials and equipment used in the study

Category	Item	Source / Manufacturer
Material	*Bacopa monnieri*	Dhanvantari Ayurvedalaya, Bibwewadi, Pune, India
Material	Poloxamer 407	Sciquant Innovations (OPC) Pvt. Ltd., Pune, India
Material	HPMC K4M	Sciquant Innovations (OPC) Pvt. Ltd., Pune, India
Material	Methanol, Ethanol (99.7%), DMSO	Analytical grade, local supplier
Material	Phosphate buffer (pH 6.8)	Laboratory-prepared, analytical grade
Material	Potassium bromide (KBr)	Shimadzu, Japan
Material	Distilled water	Laboratory-purified
Equipment	UV-Visible spectrophotometer	Shimadzu UV-1900
Equipment	Brookfield viscometer (spindle S-94)	Brookfield Engineering, USA
Equipment	Magnetic stirrer with hot plate	Remi Instruments, India
Equipment	Vial inversion system (gelling test)	Laboratory setup
Equipment	pH meter	Thermo Scientific, USA
Equipment	Incubator (antimicrobial study)	Labline Instruments, India
Equipment	Vernier caliper (spreadability)	Mitutoyo, Japan
Equipment	Franz diffusion cell apparatus	Laboratory setup

2.2 Preformulation Study: Organoleptic Evaluation

The organoleptic evaluation of *Bacopa monnieri* was carried out to assess its physical sensory characteristics. A small quantity of the pure drug was placed on a clean, dry white tile under natural daylight for visual observation, and its color was compared against a standard color reference. Odor was assessed by three independent observers in a well-ventilated room, and texture was examined by gently rubbing a small quantity of the powder between the thumb and index finger to evaluate smoothness or grittiness. All observations were performed in triplicate to ensure consistency[6].

2.3 UV Spectroscopic Method

The absorbance maxima (λmax) of *Bacopa monnieri* was determined using a UV-Visible spectrophotometer (Shimadzu UV-1900). A stock solution was prepared by dissolving 10 mg of the drug in 100 mL of methanol to obtain a concentration of 100 µg/mL, which was further diluted to 10 µg/mL. The solution was scanned over a wavelength range of 200–400 nm using methanol as blank, and the wavelength

corresponding to maximum absorbance was identified. A calibration curve was subsequently constructed at this wavelength across a range of known concentrations to confirm linearity and Beer–Lambert compliance, validating the method for drug content estimation.

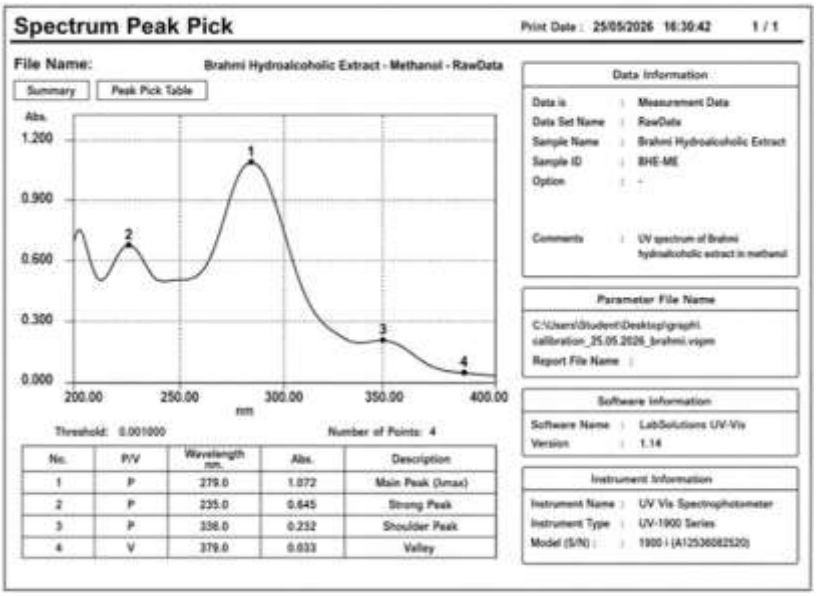

Figure 1: UV absorption spectrum of Bacopa monnieri hydroalcoholic extract in methanol, showing λmax at 279 nm

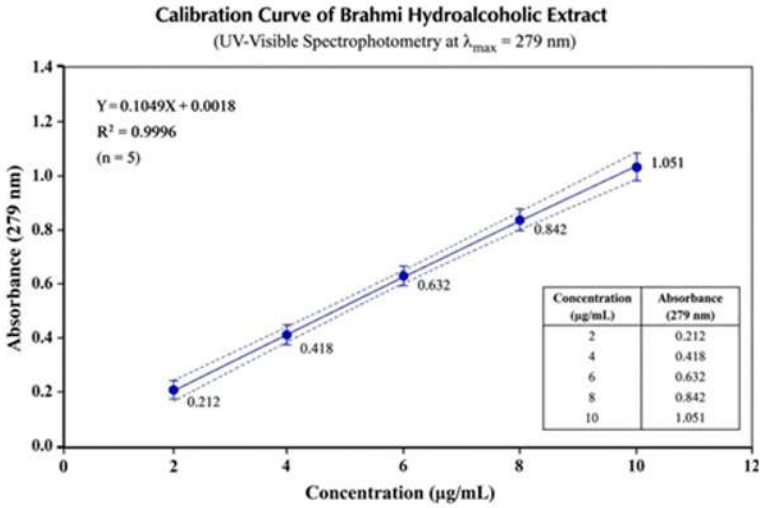

Figure 2: Calibration curve of Bacopa monnieri extract in methanol (200–400 nm scan)

2.4 . Composition of the nine formulations prepared

Ingredient	1	2	3	4	5	6	7	8	9
Bacopa monnieri (mg)	0.5	0.5	0.5	0.5	0.5	0.5	0.5	0.5	0.5
Poloxamer 407 (% w/v)	16	18	20	16	18	20	16	18	20
HPMC K4M (% w/v)	0.5	0.5	0.5	1.0	1.0	1.0	1.5	1.5	1.5
Paraben (mg)	0.02	0.02	0.02	0.02	0.02	0.02	0.02	0.02	0.02
Methanol (mL)	5	5	5	5	5	5	5	5	5
Distilled water	q.s.	q.s.	q.s.	q.s.	q.s.	q.s.	q.s.	q.s.	q.s.

2.5 Preparation of the In-Situ Thermosensitive Hydrogel

The hydrogel was prepared by the cold method[7]. Required quantities of Poloxamer 407 and HPMC K4M were weighed and kept at 4 ± 0.5 °C overnight to obtain a clear polymeric sol of the specified concentration (% w/w), with continuous stirring at 40 rpm. *Bacopa monnieri* was quantitatively weighed and dissolved in methanol to prepare the drug solution, which was then incorporated into the polymeric sol under continuous stirring at 40 rpm. The resulting hydrogel composite was subsequently characterized for its thermosensitive properties[8].

2.6 Molecular Docking

Molecular docking studies were carried out to investigate the binding interaction of Bacoside A with Vascular Endothelial Growth Factor Receptor-2 (VEGFR-2), a key regulator of angiogenesis relevant to wound healing. The crystal structure of VEGFR-2 (PDB ID: 4ASD) was selected as the target receptor and prepared by removing water molecules and non-essential atoms, adding polar hydrogen atoms, and assigning Kollman charges. Docking was performed using AutoDock 4.2 with the Lamarckian Genetic Algorithm, and a grid box was constructed around the active site (grid center X: −24.62, Y: −0.39, Z: −10.93; grid size 60 × 60 × 60 Å). Bacoside B and the reference standard Nitrofurazone were docked under identical conditions for comparison. Protocol reliability was confirmed by re-docking the native co-crystallized ligand and calculating the RMSD relative to its original pose, which was found to be within the accepted threshold for a validated docking protocol. The results demonstrated that Bacoside A effectively occupied the active site of VEGFR-2 and formed multiple stabilizing interactions with surrounding amino acid residues.

2.7 Evaluation of the In-Situ Thermosensitive Hydrogel

2.7.1 pH: The pH of the gel formulations was determined using a digital pH meter, calibrated with standard buffer solutions (pH 4.0, 7.0, and 9.2), based on measurement of hydrogen ion concentration ($pH = -\log[H^+]$). Approximately 1 g of gel was dispersed in 10 mL distilled water, and the electrode reading was allowed to stabilize for 1–2 minutes before recording. The test was repeated three times and the average pH value calculated.

2.7.2 Gelling temperature: The gelation temperature was determined by the vial inversion method. Samples were heated in a water bath at 37 °C with an increase of 1 °C per minute, and the sol–gel transition was assessed by tilting the vials at 90° at regular intervals. The temperature at which the hydrogel ceased to flow and remained stationary was recorded as the gelation temperature.

2.7.3 Gelling time: Using the vial inversion method, a 2 mL volume of formulation was heated at a controlled temperature increment and periodically tilted; the time at which the formulation ceased flowing was recorded as the gelling time.

2.7.4 Viscosity: Viscosity was determined using a Brookfield viscometer with an S-94 spindle at 100 rpm, with measurements carried out in triplicate while cooling to ensure reliability and accuracy.

2.7.5 Mucoadhesive strength: Mucoadhesive strength was measured using a modified physical balance method. Freshly excised mucosal tissue was affixed to two glass vials, with a known amount of gel applied between them and held in contact for 2 minutes. Weights were gradually added to one vial until the two separated, and

mucoadhesive strength was calculated as strength = (m × g)/A, where m is the weight required for detachment (g), g is the gravitational constant (980 cm/s²), and A is the contact area of the mucosa (cm²).

2.7.6 Spreadability: A 20 g sample of gel was spread between two glass plates subjected to a 500 g weight for 5 minutes, and the diameter of spread was measured using a caliper. The test was performed in triplicate to ensure reliable, consistent results.

2.7.7 Ex-vivo/in vitro drug release study: Drug release and permeation were evaluated using a Franz diffusion cell. A dialysis membrane was hydrated by soaking in distilled water for 12–24 h and mounted between the donor and receptor compartments, smooth side facing the donor compartment. The receptor compartment was filled with phosphate buffer (pH 7.4), maintained at 37 ± 0.5 °C, and stirred continuously at 500–600 rpm. Formulation equivalent to the required drug amount was placed in the donor compartment, which was covered with parafilm/aluminum foil to prevent evaporation. Aliquots (1–2 mL) were withdrawn at predetermined intervals (0.5, 1, 2, 4, 6, 8, 12, and 24 h) and replaced with an equal volume of fresh receptor medium to maintain sink conditions. The cumulative amount of drug permeated per unit area was calculated and plotted against time.

2.7.8 Antibacterial activity: Antimicrobial activity was evaluated by the agar well diffusion method against *Escherichia coli* and *Streptococcus* spp. using Mueller-Hinton Agar (MHA). The medium was prepared, autoclaved at 15 lbs (121 °C) for 15 minutes, and poured into petri plates. Bacterial cultures were uniformly swabbed onto the solidified agar, wells (6–8 mm) were bored using a sterile borer, and loaded with 1 mg/mL of the test extract; sterile water served as the negative control. Plates were incubated at 37 °C for 24 hours, after which the zone of inhibition around each well was measured in millimeters using a scale.

3. RESULTS AND DISCUSSION:

3.1 Organoleptic and UV Spectroscopic Characterization

Preliminary evaluation of the *Bacopa monnieri* extract was carried out to confirm its identity and quality prior to formulation. The extract exhibited a characteristic greenish colour, a distinctive characteristic odour, and a mildly bitter taste typical of the plant material (Table 4). These findings were consistent with the expected sensory profile of the crude drug and indicated the absence of gross adulteration or degradation of the starting material.

Table 4. Organoleptic properties of Bacopa monnieri extract

Parameter	Observed value
Colour	Greenish
Odour	Characteristic odour
Taste	Mildly bitter, typical of the plant

UV spectroscopic scanning of the extract in methanol (Figure 1) produced a single, sharp absorption maximum, confirming a well-defined chromophore suitable for spectrophotometric quantification. A calibration curve constructed at this wavelength (Figure 2) was found to be linear across the concentration range examined, confirming adherence to the Beer–Lambert law and validating the reliability of the method for subsequent drug-content estimation at every stage of formulation development.

3.2 Molecular Docking Study

To probe a plausible molecular basis for the wound-healing activity traditionally attributed to *Bacopa monnieri*, its two major phytoconstituents

Bacoside A and Bacoside B together with the reference drug Nitrofurazone, were docked into the active site of Vascular Endothelial Growth Factor Receptor-2 (VEGFR-2; PDB ID: 4ASD), a receptor that governs the angiogenic signalling central to the proliferative phase of wound repair.

Before evaluating the test ligands, the docking protocol itself was validated by removing the native co-crystallized ligand and re-docking it into its original binding site under identical conditions. The re-docked pose overlapped closely with the experimentally observed conformation, yielding a root-mean-square deviation (RMSD) of only 0.5 Å (Figure 3) well within the widely accepted 2 Å threshold for a validated docking protocol[10], confirming that the grid box, scoring function and search parameters employed were suitable for generating reliable binding poses for the phytoconstituents.

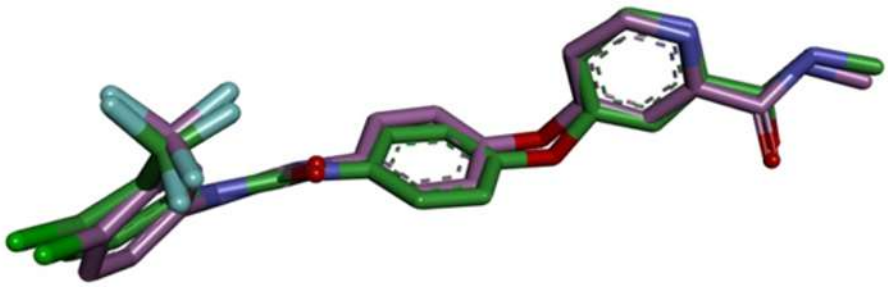

Figure 3: Overlay of re-docked and original co-crystallized ligand pose in VEGFR-2 (RMSD = 0.5 Å) docking protocol validation.

Table 5. Best binding energies obtained from AutoDock 4.2 docking against VEGFR-2 (4ASD)

Ligand	Best binding energy (kcal/mol)
Co-crystallized (native) ligand	−11.22
Nitrofurazone (standard drug)	−7.84
Bacoside A	−6.95
Bacoside B	−4.91

As expected, the native co-crystallized ligand showed the strongest binding energy (−11.22 kcal/mol), since the binding pocket is naturally shaped to accommodate it. Among the test compounds, Bacoside A bound more strongly (−6.95 kcal/mol) than Bacoside B (−4.91 kcal/mol), indicating a more stable interaction of Bacoside A with VEGFR-2. Both phytoconstituents bound less strongly than the standard drug Nitrofurazone (−7.84 kcal/mol); nevertheless, the value obtained for Bacoside A falls within a range generally regarded as reflecting a meaningful, energetically favourable interaction, indicating that Bacopa monnieri contains natural constituents capable of engaging a wound-healing-related protein target, with Bacoside A the more promising of the two.

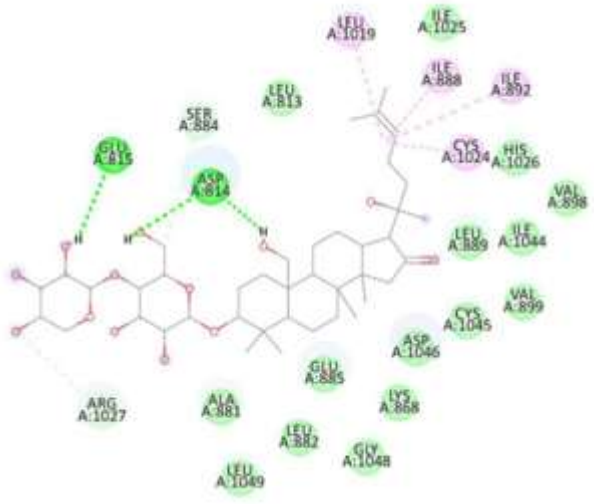

Figure 4: 2D interaction diagram of Bacoside A with amino acid residues of VEGFR-2.

Bacoside A fitted well within the VEGFR-2 active site, forming conventional hydrogen bonds with GLU815 and ASP814 (the latter forming two separate hydrogen bonds), reflecting firm anchoring of its glycoside moiety, together with a carbon–hydrogen bond with ARG1027. The molecule was further stabilized by extensive van der Waals contacts (LEU813, SER884, ALA881, LEU882, LEU1049, GLY1048, LYS868, GLU885, VAL898, VAL899, ASP1046, CYS1045, ILE1044, HIS1026, ILE1025) and alkyl interactions with LEU1019, ILE888, ILE892 and CYS1024 arising from its hydrocarbon side chain. The abundance of hydroxyl and sugar groups on Bacoside A accounts for this extensive hydrogen-bonding network and, in turn, its comparatively stronger binding energy.

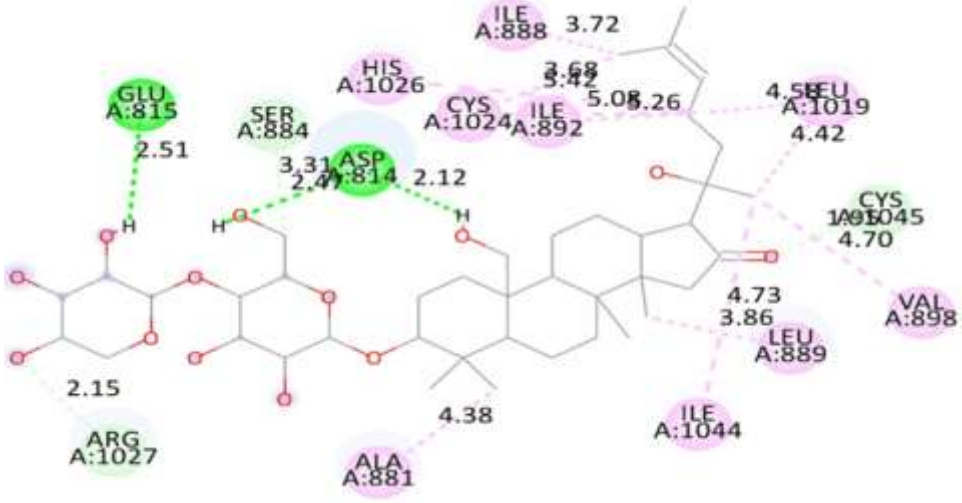

Figure 5: 2D interaction diagram of Bacoside B with amino acid residues of VEGFR-2.

Bacoside B occupied the same active-site region, forming conventional hydrogen bonds with LYS838, LYS920 and PRO839 that anchored its sugar portion, together with a Pi-Sigma interaction with PHE1047 and an alkyl interaction with ARG1051 contributed by its branched hydrocarbon side chain; additional van der Waals contacts were formed with GLU850, PHE918, GLY841, LEU840, ALA1050, ASP1052, ASP1056, LYS1055 and ARG842. Despite its close structural similarity to Bacoside A, Bacoside B formed fewer strong hydrogen bonds and achieved a somewhat less tight fit within the pocket, consistent with its weaker binding energy. For comparison, the standard drug Nitrofurazone a smaller, more rigid molecule formed conventional hydrogen bonds with GLU917, CYS919 and ASP1046, a Pi-Sulfur interaction with CYS1045, a Pi-Pi T-shaped interaction with PHE1047, and Pi-Alkyl contacts with VAL899, VAL848 and VAL916 (interaction diagram provided as supplementary data), packing more tightly into the pocket through several stabilizing ring-based interactions that the bulkier glycosides could not form as efficiently, which accounts for its comparatively stronger binding energy relative to the two phytoconstituents.

Taken together, the order of binding strength observed was: native ligand (−11.22 kcal/mol) > Nitrofurazone (−7.84 kcal/mol) > Bacoside A (−6.95 kcal/mol) > Bacoside B (−4.91 kcal/mol), generated using a validated docking protocol (RMSD 0.5 Å). Although the phytoconstituents bound somewhat less strongly than the standard drug, both occupied the same active-site pocket of VEGFR-2 and formed multiple hydrogen bonds

and hydrophobic contacts with key residues, indicating a real and specific interaction rather than a weak, random fit. Because VEGFR-2 governs the angiogenic signalling required to supply the proliferating wound bed with oxygen, nutrients and immune cells[11], the ability of Bacoside A and Bacoside B to engage this receptor suggests a plausible molecular contribution to the wound-healing property of *Bacopa monnieri*. Docking alone, however, predicts only the strength and pattern of binding; confirmation of the resulting biological effect on receptor activity will require further studies such as molecular dynamics simulations, receptor-binding assays, or in vitro/in vivo angiogenesis and wound-healing models. The present results nonetheless provide encouraging, mechanism-based support for the traditional use of *Bacopa monnieri* in wound care and identify Bacoside A as the principal active constituent of interest.

3.3 Physicochemical Characterization of Batches F1–F3

Three representative batches (F1, F2 and F3), selected from the 3^2 factorial design, were evaluated for pH, viscosity, gelation temperature, gelling time, spreadability and mucoadhesive strength; the consolidated results are presented in Table 6.

Table 6. Consolidated physicochemical characterization of hydrogel batches F1, F2 and F3

Parameter	F1	F2	F3
pH (mean)	6.73	6.53	6.86
Viscosity (cP, 20 rpm)	31,000	24,000	27,500
Gelation temperature (°C)	34.2	37.5	35.8
Gelling time (s, at 37 ± 1 °C)	42	58	49
Spreadability (g·cm/s)	15.5	23.6	19.4
Mucoadhesive strength (dyne/cm²)	4120	3250	3680

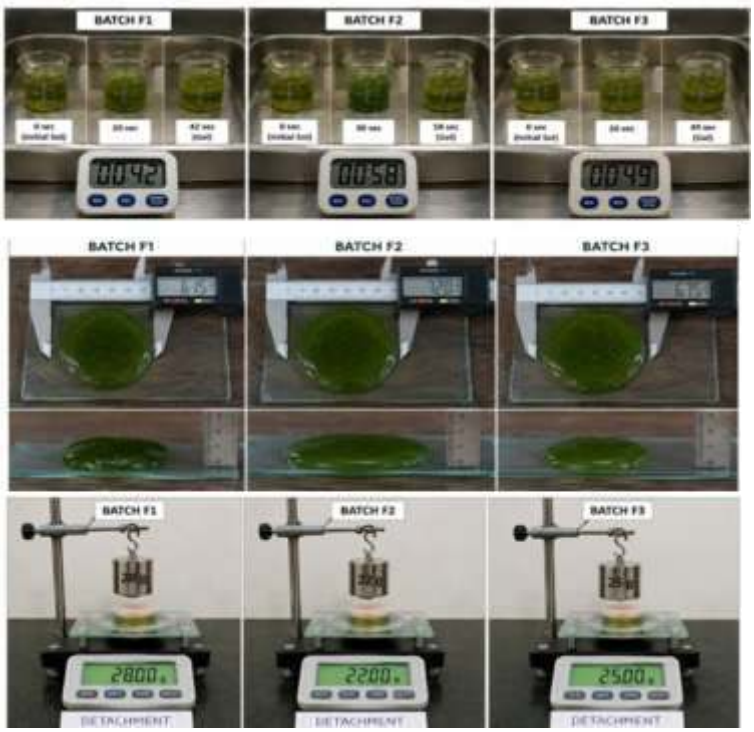

Figure 6: Comparative physicochemical profile of hydrogel batches F1, F2, and F3 (gelling time, spreadability, mucoadhesive strength).

All three batches showed pH values within the skin-friendly range (approximately 5.5–7.0), with F2 slightly more acidic and F1 and F3 closer to neutral; none of the formulations would be

expected to irritate intact or wounded skin on application. Viscosity was inversely related to spreadability: F1, containing the lowest HPMC K4M level relative to its polymer ratio, showed the highest viscosity (31,000 cP), consistent with a firmer gel network, while F2 showed the lowest viscosity (24,000 cP) and correspondingly the greatest spreadability (23.6 g·cm/s); F3 occupied an intermediate position (27,500 cP; 19.4 g·cm/s), reflecting a good balance between consistency and ease of application. Gelation temperature and gelling time arguably the most critical parameters for an in-situ system, since the formulation must remain a free-flowing sol at room temperature but transition rapidly to a gel at skin/body temperature were acceptable for all three batches, ranging from 34.2–37.5 °C and 42–58 s, respectively; F1 gelled fastest owing to its higher effective polymer concentration, whereas F2 gelled more slowly but yielded a smoother texture, and F3 (35.8 °C; 49 s) again occupied an optimal intermediate position, being neither so fast as to risk air entrapment and uneven application nor so slow as to risk run-off from the wound bed before setting. Mucoadhesive strength followed a pattern broadly consistent with viscosity, with F1 showing the strongest adhesion (4120 dyne/cm²), F3 good adhesion (3680 dyne/cm²), and F2 the lowest (3250 dyne/cm²); all three values nonetheless indicate satisfactory retention capability at the intended application site.

3.4 Selection of the Optimized Batch (F3)

Although F1 exhibited the highest viscosity and mucoadhesive strength, and F2 offered the fastest spreadability, batch F3 was selected as the optimized formulation for further biological evaluation on the basis of its overall balanced profile combined with superior functional performance. Its gelation temperature (35.8 °C) and gelling time (49 s) fell between the extremes represented by F1 (rapid, potentially premature gelation) and F2 (slower, less convenient handling), providing a sol–gel transition well matched to practical application at the wound site. Its viscosity (27,500 cP) and mucoadhesive strength (3680 dyne/cm²) were both good rather than extreme, supporting adequate wound-site retention without compromising spreadability, and its pH (6.86) remained comfortably within the skin-friendly range. Critically, this balanced physical profile was accompanied by the strongest functional read-outs of the three batches: F3 produced both the largest zone of inhibition against Escherichia coli (22 mm; Section 3.5) and the highest cumulative in vitro drug release (97.5% at 24 h; Section 3.6), indicating that its higher polymer loading (20% w/v Poloxamer 407, 1.5% w/v HPMC K4M) did not compromise and, if anything, enhanced drug release and antibacterial performance relative to the other batches. On this basis, F3 was selected as the optimized batch carried forward for correlating formulation design with therapeutic-relevant outcomes.

3.5 Antimicrobial Activity

Because infection is a major obstacle to normal wound healing, the antibacterial potential of the formulations was evaluated by the agar well diffusion method against Escherichia coli (Gram-negative) and Streptococcus spp. (Gram-positive), two organisms commonly associated with wound infection.

Table 7. Zone of inhibition (mm) of the standard drug and formulations against Escherichia coli

Sample	Zone of inhibition (mm) at 1 mg/mL
Control	NA
Standard drug	14
F1	15
F2	18
F3	22

Table 8. Zone of inhibition (mm) of the crude extract and formulations against Streptococcus spp.

Sample	Zone of inhibition (mm) at 1 mg/mL
Control	NA
Crude extract (powder)	12
F1	13
F2	17
F3	16

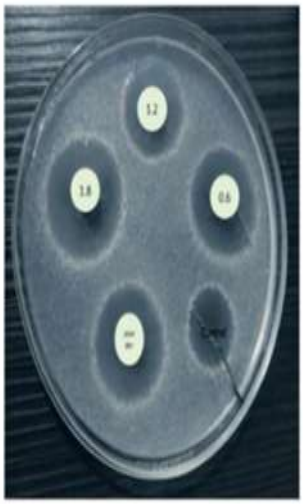

Figure 7: Zone of inhibition of standard drug and formulations (F1–F3) against Escherichia coli and Streptococcus spp.

The negative control showed no zone of inhibition against either organism, confirming the validity of the assay. Against E. coli, all three gel batches outperformed the standard drug, with inhibition increasing steadily from F1 to F3; F3 produced the largest zone (22 mm), exceeding even the standard, indicating good intrinsic antibacterial activity of the *Bacopa monnieri* extract that is most pronounced in the F3 formulation. A similar trend was observed against Streptococcus spp., where the formulated gels again outperformed the plain crude extract, with F2 and F3 producing the largest, closely comparable zones (17 and 16 mm, respectively) indicating that incorporation into the gel matrix does not diminish, and appears to enhance, antibacterial action, most likely by maintaining prolonged contact between the active constituents and the bacterial culture. Collectively, these results confirm that the developed hydrogel possesses antibacterial activity against both Gram-negative and Gram-positive organisms, supporting its intended role in controlling infection at the wound site an essential requirement of any topical wound-healing formulation.

3.6 In Vitro Drug Diffusion Study

The in vitro release and permeation behaviour of the three batches was evaluated using a Franz diffusion cell over 24 h, with the optimized formulation expected to show maximum cumulative release with sustained permeation and higher flux, characteristics considered desirable for a topical delivery system.

Table 9. Cumulative in vitro drug release (%) of hydrogel batches F1, F2 and F3 using a Franz diffusion cell (mean ± SD, n = 3)

Time (h)	F1 (%)	F2 (%)	F3 (%)
0.5	12.4 ± 0.5	15.2 ± 0.4	18.6 ± 0.6
1	20.8 ± 0.7	25.6 ± 0.5	31.4 ± 0.8
2	32.5 ± 0.8	39.7 ± 0.7	47.8 ± 0.9
4	45.3 ± 0.9	54.8 ± 0.8	65.2 ± 1.1
6	56.7 ± 1.0	66.4 ± 0.9	76.9 ± 1.2
8	65.9 ± 1.1	75.8 ± 1.0	85.6 ± 1.3
12	74.6 ± 1.2	84.3 ± 1.1	92.8 ± 1.4
24	82.1 ± 1.3	90.7 ± 1.2	97.5 ± 1.5

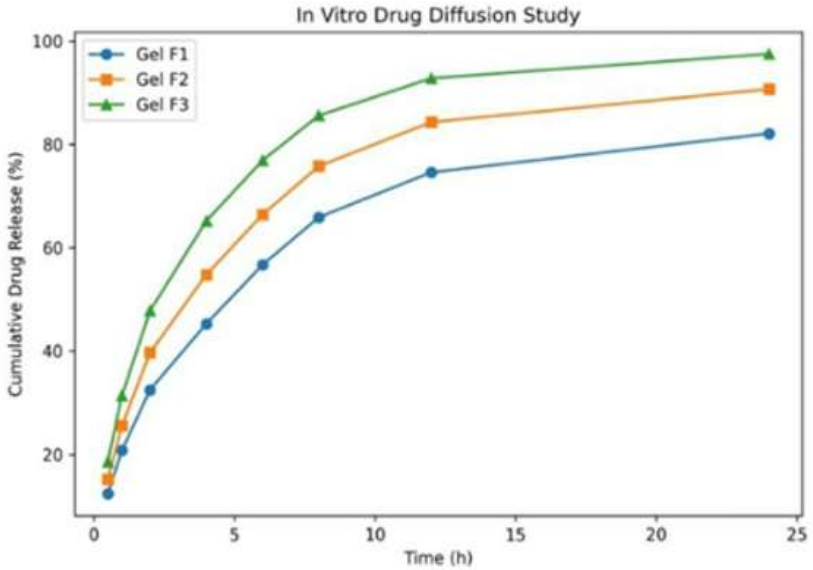

Figure 8: Cumulative in vitro drug release (%) profile of hydrogel batches F1, F2, and F3 over 24 hours (Franz diffusion cell).

Cumulative release increased progressively across all three batches over the 24 h study period, with F3 consistently outperforming F1 and F2 at every time point, reaching 97.5 ± 1.5% at 24 h compared with 90.7 ± 1.2% for F2 and 82.1 ± 1.3% for F1. The comparatively modest release recorded at 0.5 h (12.4–18.6%) across all batches indicates the absence of an uncontrolled burst effect, while the steady, near-linear increase thereafter reflects a sustained-release profile appropriate for a topical wound dressing intended to provide prolonged therapeutic action at the application site. The release rank order (F3 > F2 > F1) mirrors the trend observed in the antimicrobial data (Section 3.5) and is consistent with the balanced viscosity and mucoadhesive profile of F3 (Section 3.3–3.4), further reinforcing its selection as the lead formulation.

3.7 Overall Discussion

The molecular docking study provided a plausible mechanistic rationale for the traditional wound-healing use of *Bacopa monnieri*, demonstrating that its major phytoconstituents particularly Bacoside A can engage the angiogenesis-related receptor VEGFR-2 through a validated docking protocol (RMSD 0.5 Å), forming multiple specific hydrogen-bonding and hydrophobic interactions within the same active-site pocket occupied by the standard drug. Independently, the physicochemical characterization confirmed that all three prepared batches met the essential criteria for a thermosensitive in-situ hydrogel skin-compatible pH, appropriate viscosity, and a sol–gel transition triggered close to physiological temperature while batch F3 offered the most favourable balance of handling properties. This formulation-level advantage was corroborated by two independent functional read-outs: F3 produced the largest antibacterial zones of inhibition against a representative Gram-negative organism (E. coli) and comparably strong activity against a Gram-positive organism (Streptococcus spp.), and it also delivered the highest and most sustained cumulative drug release over 24 h. The convergence of these independent lines of evidence computational, physicochemical, microbiological and biopharmaceutical on batch F3 substantially strengthens confidence in its selection as the lead candidate, rather than resting on any single parameter in isolation.

These findings directly support the translational rationale outlined in the Introduction. Conventional topical wound-care systems are limited by poor site retention, uneven distribution, and inadequate moisture regulation, while relying largely on synthetic actives that can irritate already compromised tissue[12]. The thermosensitive in-situ hydrogel developed here addresses these limitations through a free-flowing sol that converts to a mucoadhesive gel on contact with the skin, while simultaneously delivering a multifunctional phytotherapeutic agent whose antioxidant, anti-inflammatory, antimicrobial, and as suggested by the present docking results pro-angiogenic activities converge on the same wound-healing target. Taken together, the optimized F3 formulation represents a proof-of-concept translational candidate that bridges rational formulation engineering with the multifunctional bioactivity of *Bacopa monnieri*, warranting further mechanistic validation (e.g., molecular dynamics simulations, receptor-binding assays) and in vivo wound-healing studies to confirm its clinical translational potential.

4. CONCLUSION:

The present study successfully developed and characterized a thermosensitive in-situ hydrogel incorporating *Bacopa monnieri* for topical wound-healing application. Among the three batches evaluated, F3 (20% w/v Poloxamer 407, 1.5% w/v HPMC K4M) emerged as the optimized formulation, offering a well-balanced sol–gel transition (35.8 °C; 49 s), good viscosity and mucoadhesive strength, and a skin-compatible pH, without compromising ease of application. This formulation-level balance translated into superior functional performance: F3 delivered the highest and most sustained cumulative drug release (97.5% at 24 h) among the batches tested, indicating its suitability for prolonged therapeutic action at the wound site, and produced the largest antibacterial zones of inhibition against *Escherichia coli*, with comparably strong activity against *Streptococcus* spp., confirming broad-spectrum efficacy against both Gram-negative and Gram-positive wound pathogens. Molecular docking of the major phytoconstituents against VEGFR-2 (validated with an RMSD of 0.5 Å) further provided a plausible mechanistic basis for this bioactivity, with Bacoside A showing the more favourable binding profile and identifying it as the principal constituent of interest. Taken together, these convergent computational, physicochemical, microbiological, and biopharmaceutical findings position the optimized F3 hydrogel as a promising phytotherapeutic alternative to conventional synthetic wound dressings, combining sustained drug delivery, antimicrobial protection, and a rational molecular basis for efficacy within a single, patient-friendly platform. Further validation through molecular dynamics simulations, receptor-binding assays, and in vivo/preclinical wound-healing studies is warranted to confirm the translational and clinical potential of this formulation.

Based on the topics your Introduction covers (wound-healing physiology, limitations of conventional wound care, in-situ thermosensitive hydrogels, *Bacopa monnieri* pharmacology, and the supporting methodology — factorial design, UV validation, Franz diffusion, docking, antimicrobial testing), here is a master reference list of real, peer-reviewed sources in Vancouver style (plain numbered text, ready to paste into your References section).

REFERENCES

1. Almadani YH, Vorstenbosch J, Davison PG, Murphy AM. Wound healing: a comprehensive review. Semin Plast Surg. 2021;35(3):141–144.

2. Soliman AM, Das S, Abd Ghafar N, Teoh SL. Role of microRNA in proliferation phase of wound healing. Front Genet. 2018;9:38.
3. Landén NX, Li D, Ståhle M. Transition from inflammation to proliferation: a critical step during wound healing. Cell Mol Life Sci. 2016;73(20):3861–3885.
4. Barrientos S, Stojadinovic O, Golinko MS, Brem H, Tomic-Canic M. Growth factors and cytokines in wound healing. Wound Repair Regen. 2008;16(5):585–601.
5. Velnar T, Bailey T, Smrkolj V. The wound healing process: an overview of the cellular and molecular mechanisms. J Int Med Res. 2009;37(5):1528–1542.
6. Broughton G 2nd, Janis JE, Attinger CE. Wound healing: an overview. Plast Reconstr Surg. 2006;117(7 Suppl):1e–S32e.
7. Diegelmann RF. Analysis of collagen synthesis. Methods Mol Med. 2003;78:349–358.
8. Bao P, Kodra A, Tomic-Canic M, Golinko MS, Ehrlich HP, Brem H. The role of vascular endothelial growth factor in wound healing. J Surg Res. 2009;153(2):347–358.
9. Shams F, Moravvej H, Hosseinzadeh S, Mostafavi E, Bayat H, Kazemi B, et al. Overexpression of VEGF in dermal fibroblast cells accelerates the angiogenesis and wound healing function: in vitro and in vivo studies. Sci Rep. 2022;12:18701.
10. Hostler A, et al. Decoding wound healing: cellular insights and technological advances. NPJ Biomed Innov. 2025.
11. Enhancing wound healing dressing development through interdisciplinary collaboration. Int J Mol Sci. 2021.
12. Sharath R, Harish BG, Krishna V, Sathyanarayana BN, Swamy HMK. Wound healing and protease inhibition activity of Bacoside-A, isolated from Bacopa monnieri Wettest. Phytother Res. 2010;24(8):1217–1222.
13. Murthy S, Gautam MK, Goel S, Purohit V, Sharma H, Goel RK. Evaluation of in vivo wound healing activity of Bacopa monniera on different wound model in rats. Biomed Res Int. 2013;2013:972028.
14. Valotto Neto LJ, de Araujo MR, Moretti Junior RC, Machado NM, Joshi RK, dos Santos Buglio D, et al. Investigating the neuroprotective and cognitive-enhancing effects of Bacopa monnieri: a systematic review focused on inflammation, oxidative stress, mitochondrial dysfunction, and apoptosis. Antioxidants. 2024;13(4):393.
15. Manap AS, Vijayabalan S, Madhavan P, Chia YY, Arya A, Wong EH, et al. Bacopa monnieri, a neuroprotective lead in Alzheimer disease: a review on its properties, mechanisms of action, and preclinical and clinical studies. Drug Target Insights. 2019;13:1177392819866412.
16. Fazlul MKK, Deepthi SP, Irfan M. Antibacterial and antifungal activity of various extracts of Bacopa monnieri. Int J Pharm Res. 2019;11:1698–1702.
17. Bacopa monnieri phytochemicals regulate fibroblast cell migration via modulation of focal adhesions. Sci Rep / J Ethnopharmacol. 2024.
18. Assessing the anti-inflammatory effects of Bacopa-derived bioactive compounds using network pharmacology and in vitro studies. ACS Omega. 2022.
19. Kaushal M, et al. (topical/phytotherapeutic wound-care context). In: Phytochemicals and naturally derived substances for wound healing. Adv Wound Care (New Rochelle). 2013.
20. Chen J, et al. An update of phytotherapeutic advances of marigold (Calendula officinalis L.) in wound healing. Pharmaceuticals (Basel). 2025.
21. Phytotherapeutic insights into wound healing: unveiling the potential of Agrimonia eupatoria L. Phytochem Rev. 2025.
22. Süntar I, Akkol EK, Nahar L, Sarker SD. Wound healing and antioxidant properties: do they coexist in plants? Free Radic Antioxid. 2012.
23. Skin wound healing and phytomedicine: a review. Pharmacology. 2014;93(1-2):71–82.
24. Kwiecień I, et al. Poloxamer 407 as a component of thermosensitive in-situ hydrogel systems: a review of pharmaceutical

and pharmacological characteristics. Pharmaceutics. 2021.
25. New biopharmaceutical characteristics of in situ systems based on poloxamer 407. Gels. 2023;9(7):508.
26. In situ forming poloxamer-based thermo-sensitive hydrogels for ocular application: a focus on the derivatives 407 and 188. Gels. 2025;11(9):752.

HOW TO CITE: Pratima Sagar, Sharavari Chavan, Dr. Hemlata Wadkar, Dr. Varsha Patil, Dr. Trupti Tuse, To Develop and Optimize Bacopa monnieri in Situ Thermosensitive Hydrogel for The Treatment of Acute Wound Healing, Int. J. of Pharm. Sci., 2026, Vol 4, Issue 9, 374-389. https://doi.org/10.5281/zenodo.22247225